

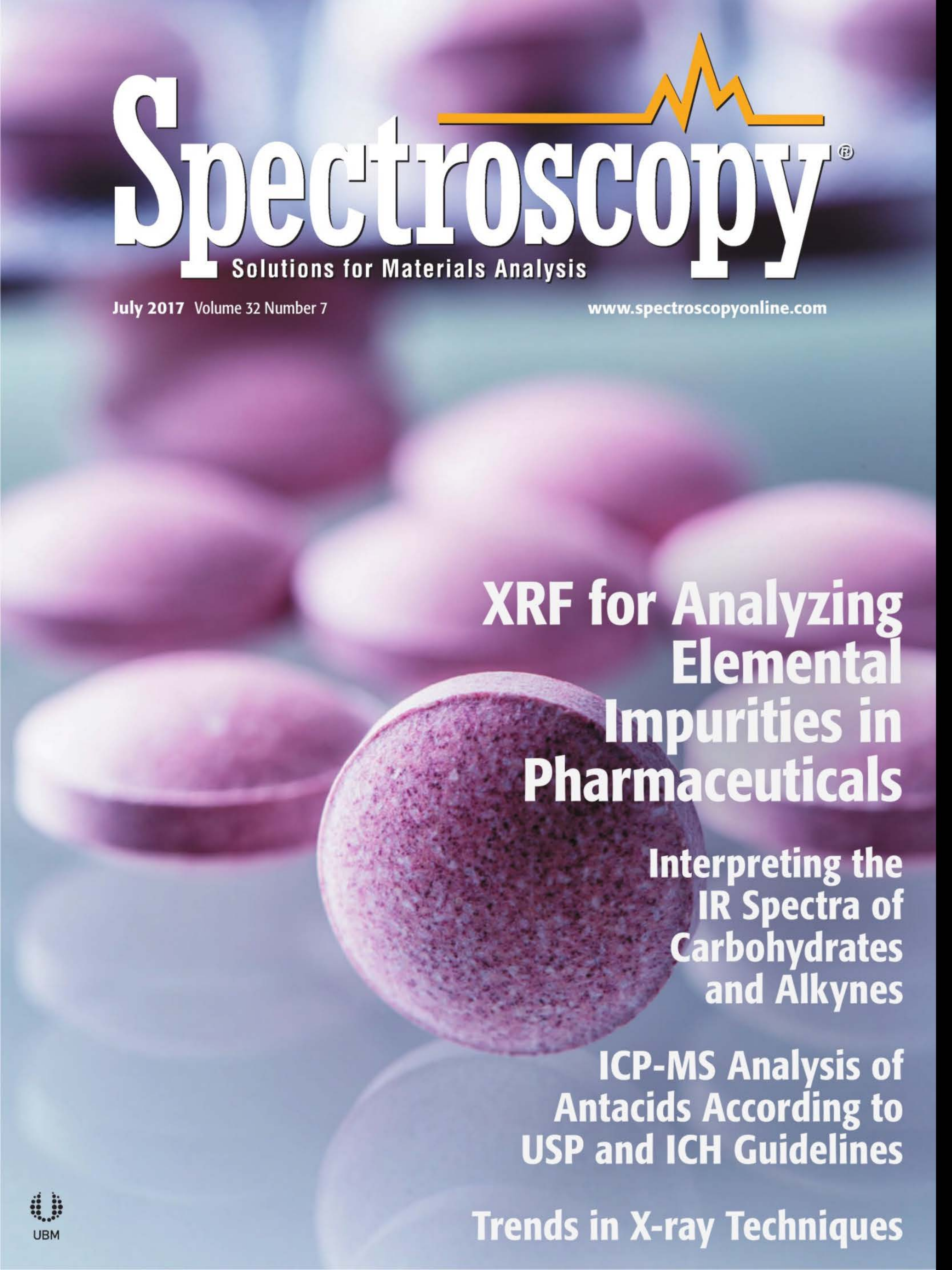


# Spectroscopy<sup>®</sup>

Solutions for Materials Analysis

July 2017 Volume 32 Number 7

[www.spectroscopyonline.com](http://www.spectroscopyonline.com)



## XRF for Analyzing Elemental Impurities in Pharmaceuticals

### Interpreting the IR Spectra of Carbohydrates and Alkynes

### ICP-MS Analysis of Antacids According to USP and ICH Guidelines

### Trends in X-ray Techniques

stub. The microcalorimeter detector has a resolution of around 5 eV and 16 individual pixels each collecting a full spectrum. The individual spectra from each pixel were summed to obtain increased counting statistics for more accurate peak position measurements.

In examining the collected spectra for the materials mentioned, it was noted that the peaks are all downshifted from the expected 282 eV position. Secondly, each of the peaks has a distinct position and differences in shape indicating differences in the  $sp^2$ - $sp^3$  ratio for each material. A Gaussian fit to the peaks provides the peak positions. Using the amorphous carbon as the carbon reference point, the nanodiamond shows the largest shift toward higher energy relative to amorphous carbon. The graphite shows a small negative shift toward lower energy relative to amorphous carbon. The soot sample appears to be the most similar to the amorphous carbon, but does exhibit a small positive shift indicating potential nanodiamond character.

Preliminary theoretical simulations of the XES of these materials using the transition potential approximation in density functional theory indicate similar trends in both the shape and position of the peaks, and support the experimental measurements. We used simple molecular models for the systems of interest that are representative of the different local environments found around the excited centers. The theoretical results predict a clear relation between the shift relative to the graphite peak and the local out-of-plane distortion around

the absorbing center, a quantity that is closely related to its  $sp^2$ - $sp^3$  character.

X-ray photoelectron spectroscopy provides the  $sp^2$ - $sp^3$  hybridizations through bombardment of the sample surface with X-rays that cause the subsequent release of electrons with the characteristic bonding energy of carbon:  $sp^2$  at 284 eV and  $sp^3$  at 285 eV. Graphite samples show purely  $sp^2$  character, and nanodiamond shows a mixture of  $sp^2$ - $sp^3$  (26–39%). The soot sample is a majority 67%  $sp^2$  with 16%  $sp^3$  character. Raman spectroscopy provides further information as to the  $sp^2$  allotropes and surface functionalization.

The microcalorimeter detector offers new X-ray measurement capabilities not found with conventional synchrotrons in that full spectra are measured compared with limited XANES scan ranges from synchrotron measurements. In addition, these measurements can be done within your laboratory.

## References

- (1) K. McIntosh, G. Havrilla, M. Croce, R. Huber, D. Podlesak, M. Rabin, F. Vila, M. Carpenter, and R. Cantor, "Study of Carbon Bonding with XES Using a TES Microcalorimeter Detector," to be presented at the 2017 Denver X-Ray Conference, Big Sky, Montana.

**Kathryn McIntosh, George J. Havrilla, Mark Croce, Rachel Huber, David Podlesak, and Michael Rabin** are with Los Alamos National Laboratory in Los Alamos, New Mexico. **Fernando Vila** is with the University of Washington, Seattle, Washington. **Matthew Carpenter and Robin Cantor** are with Star Cryoelectronics in Santa Fe, New Mexico.

## Making X-ray Fluorescence Movies in the Laboratory Using CCD and CMOS Cameras

*Kenji Sakurai and Wenyang Zhao*

For many years, viewing elements as they move in chemical systems has been a dream for scientists. Because chemical reactions are coupled with the transportation and redistribution of elements, such a capability would be an excellent tool for elucidating many unknown phenomena in pure sciences as well as in medical and industrial applications. X-ray fluorescence (XRF) is a powerful nondestructive technique for determination of chemical composition. So far, however, capturing moving images with XRF, particularly in the laboratory, has been extremely challenging. Although we have reported the creation of some XRF movies using highly brilliant synchrotron sources (1,2), it is extremely important to enable similar experiments in ordinary laboratories, schools, industries, and hospitals. This year, at the Denver X-ray Conference, we will report our latest progress toward this goal (3,4).

Roughly speaking, in XRF, one can choose either a wavelength-dispersive X-ray spectrometer, which uses an analyzing crystal, or an energy-dispersive spectrometer equipped with a semiconductor detector such as a silicon drift detector. In XRF still-imaging, one typically uses an energy-dispersive spectrometer to obtain XRF spectra ef-

**HITACHI**  
Inspire the Next

Hitachi provides comprehensive laboratory solutions, serving your needs inside AND outside the lab.

Contact us about our Summer Specials!

**Think Outside the Lab**

Spectroscopy      X-ray Fluorescence      Thermal Analysis

Hitachi High-Technologies Science America, Inc.  
www.hitachi-hightech.com Tel. 1-800-548-9001

ficiently, while scanning the sample position with a small X-ray beam (created by using a focusing device such as mono- or polycapillary optics). The measurement time to obtain each individual image is quite long, and large pixel numbers are essential to provide enough information. In this situation, movie XRF imaging looks difficult. How can one collect many such XRF images as a function of time?

The key is to change the XRF imaging strategy. We propose a new approach, which we call projection-type XRF imaging, in contrast to scanning-type imaging. In this approach, instead of making xy scans with a micro X-ray beam, we use a rather large beam to illuminate the whole sample area. All XRF data are collected by an energy-dispersive two-dimensional (2D) detector. To project an XRF image onto the 2D detector plane, we have two options: parallel optics based on a collimator plate, or a simple pinhole camera. One of the remaining problems was how to make a 2D X-ray detector that has a large number of tiny pixels with sufficient energy resolution in the X-ray wavelength region.

There has been great progress in X-ray detectors. In the present research, we are using cooled charge-coupled-device (CCD) and complementary-metal-oxide-semiconductor (CMOS) cameras, which are designed for visible light applications. It is possible that other advanced 2D X-ray detectors could be used for XRF imaging, but we believe that the use of commercially available cooled CCD and

CMOS cameras would be extremely convenient for many users, because they are not very expensive and are easy to obtain. One needs to remove the optical lenses as well as any covers, and affix an X-ray window there instead. The inside of the camera should be evacuated or at least replaced by dried gas because of the necessity of cooling.

Then the most likely next question is how to obtain X-ray energy information, which is absolutely necessary for XRF. In XRF instruments, as in other semiconductor detectors, X-ray photons create a large number of charges in a CCD or CMOS camera. Because the amount of charge corresponds to the energy of the X-rays, one can obtain information on impinged X-ray energy. This means that the intensity corresponds to the X-ray energy, if the image is read sufficiently quickly to avoid counting overlapped events. Such quick reading is often called single-photon counting. However, there are still some technical challenges. X-ray photons might not arrive at the center of the single pixel; for example, they may hit the corner of the pixel, in which case the created charges are eventually split into several pixels. Such events become more apparent when the pixel is small, particularly in the case of CCD and CMOS cameras made for visible light cameras. To deal with this problem of charge-sharing events, we are proposing a clever and fast filtering scheme.

At the 2017 Denver X-ray Conference, we will present our latest scientific XRF movies. For this work, we used a 1.5-kW



## Portable Raman for Measurements Through Opaque Packaging

The all new **i-Raman<sup>®</sup> Pro ST** provides easy identification of materials through a variety of packaging and barrier layers!

Learn More About the **i-Raman Pro ST**

[www.bwtek.com/ProSeeThrough](http://www.bwtek.com/ProSeeThrough)

[marketing@bwtek.com](mailto:marketing@bwtek.com)

+1-302-368-7824

X-ray tube. The typical energy resolution of our system is around 150 eV@MnK $\alpha$  (depending on the cooling temperature). The spatial resolution is adjustable; we typically set it at 20–50  $\mu\text{m}$ , depending on the XRF intensity of the sample. The time resolution for the movie is still not fast like a synchrotron experiment; it is on the order of a minute.

In our presentation, we will provide successful examples that visualize the real-time diffusion of elements such as calcium and iron in some chemical systems, from the beginning of the reaction to the end. One can understand how diffusion proceeds and how it depends on the element and matrix in real time. We hope this work will help to clarify the mechanism of chemical functions and reactions on a specific time scale. This novel XRF movie technique has the potential to open a new era of chemical science.

## High-Resolution X-ray Asymmetrical Reciprocal Space Mapping: A Technique for Structural Characterization of Semiconductor Superlattices

Andrian Kuchuk

Semiconductor superlattices (SLs), due to their unique electronic and transport properties, are nowadays commonly used for innovative optoelectronic devices and for high-frequency power electronics. Basically, SLs consist of a pe-

## References

- (1) K. Sakurai and H. Eba, *Anal. Chem.* **75**, 355–359 (2003). <http://dx.doi.org/10.1021/ac025793h>.
- (2) K. Sakurai and M. Mizusawa, AIP Conference Proceedings 705 (Synchrotron Radiation Instrumentation 2003, San Francisco), pp. 889–892 (2004). <http://doi.org/10.1063/1.1757938>.
- (3) W. Zhao and K. Sakurai, *Sci. Rep.* **7**, 45472 (2017). <http://dx.doi.org/10.1038/srep45472>.
- (4) W. Zhao and K. Sakurai, *Rev. Sci. Instrum.* **88**, 063703 (2017). <http://dx.doi.org/10.1063/1.4985149>.

**Kenji Sakurai, PhD**, is the managing researcher at the Research Center for Advanced Measurement and Characterization at the National Institute for Materials Science in Ibaraki, Japan. **Wenyang Zhao** is a graduate student at the University of Tsukuba in Tsukuba, Japan.

riodic arrangement of two semiconductor materials with different energy band gaps, with the SL period ( $T_{\text{SL}}$ ) much larger than the semiconductor lattice constants. Because of the quantum size effects, the miniband structure of the SL depends not only on the semiconductors band gap, but also on the geometrical design of the SL. The properties of such quantum structures can be tuned in a wide range by changing the SL period, thicknesses, and strain state of quantum well (QW)–barrier layers. High-resolution X-ray diffraction (HR-XRD) is the main tool used to determine the superstructure parameters mentioned above. Com-



**Starna**

NEW  
USP 857  
REFERENCES

ISO/IEC 17025 & ISO Guide 34 Accredited  
Simple UV/VIS/NIR Validation  
Permanently sealed cells for repeat use  
Absorbance, Stray Light,  
Wavelength, Resolution  
NIST Traceable

## Certified Reference Materials



**Starna Cells, Inc.**  
PO Box 1919 Atascadero, CA 93423  
Phone: (800) 228-4482 USA or (805) 466-8855 outside USA  
[sales@starnacells.com](mailto:sales@starnacells.com) [www.starnacells.com](http://www.starnacells.com)

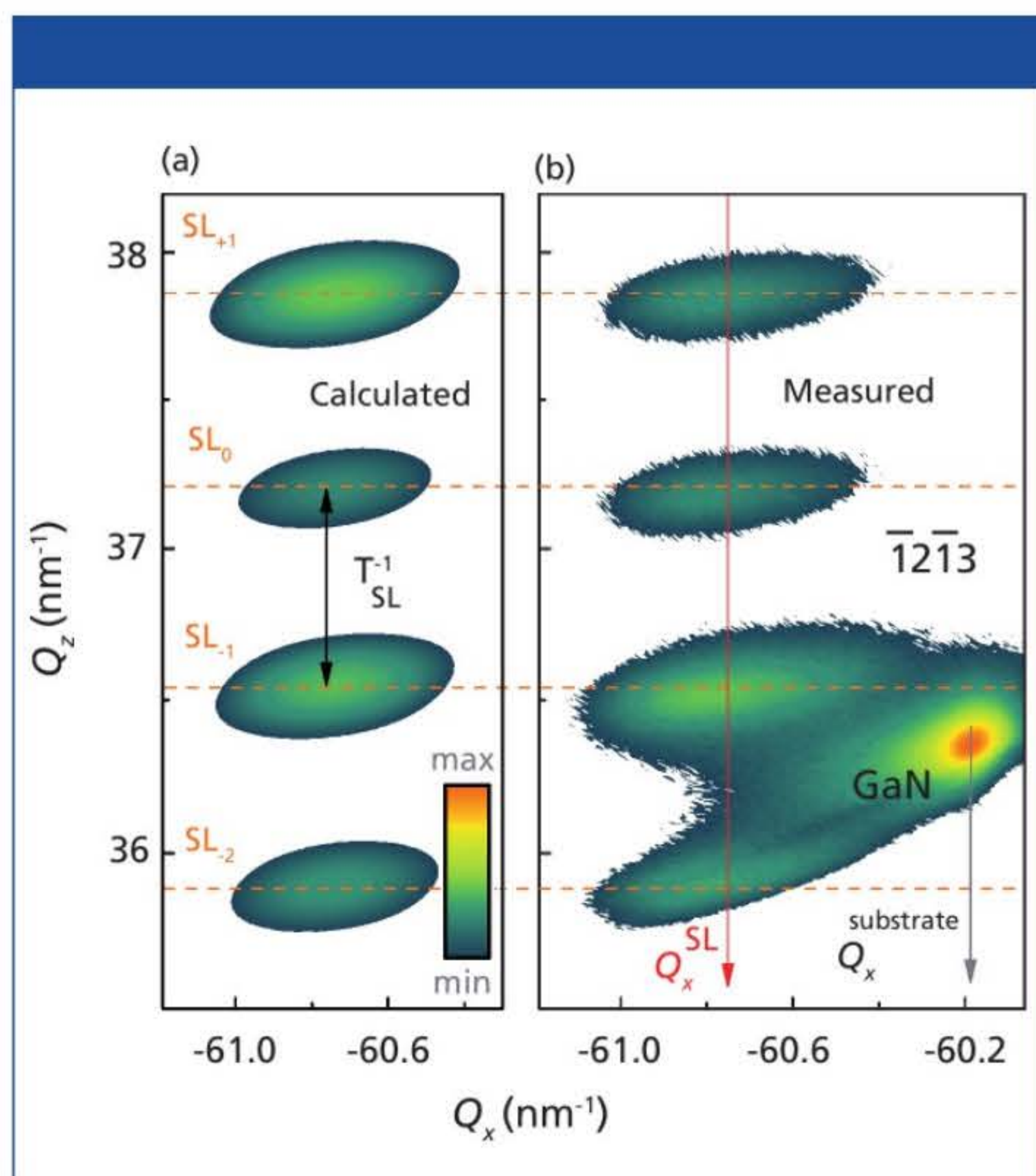


**Figure 1:** (a) Calculated and (b) measured  $\bar{1}2\bar{1}3$  RSMs for 20 periods GaN–AlN SLs with the following superstructure parameters:  $T_{\text{SL}} = 9.46$  nm;  $t_{\text{GaN}}/t_{\text{AlN}} = 4.38/5.08$  nm;  $\varepsilon_x(\text{GaN–AlN}) = -3.05 \times 10^{-3}/1.58 \times 10^{-3}$ ;  $N_{\text{TD}} = 3.32 \times 10^8 \text{ cm}^{-2}$ . The intensity is plotted in logarithmic scale.